

Optical Microfluidic Waveguides and Solution Lasers of Colloidal Semiconductor Quantum Wells

Joudi Maskoun, Negar Gheshlaghi, Furkan Isik, Savas Delikanli, Onur Erdem, Emine Yegan Erdem,* and Hilmi Volkan Demir*

The realization of high-quality lasers in microfluidic devices is crucial for numerous applications, including biological and chemical sensors and flow cytometry, and the development of advanced lab-on-chip (LOC) devices. Herein, an ultralow-threshold microfluidic single-mode laser is proposed and demonstrated using an on-chip cavity. CdSe/CdS@Cd_xZn_{1-x}S core/crown@gradient-alloyed shell colloidal semiconductor quantum wells (CQWs) dispersed in toluene are employed in the cavity created inside a poly(dimethylsiloxane) (PDMS) microfluidic device using SiO₂-protected Ag mirrors to achieve in-solution lasing. Lasing from such a microfluidic device having CQWs solution as a microfluidic gain medium is shown for the first time with a record-low optical gain threshold of 17.1 μJ cm⁻² and lasing threshold of 68.4 μJ cm⁻² among all solution-based lasing demonstrations. In addition, air-stable SiO₂ protected Ag films are used and designed to form highly tunable and reflective mirrors required to attain a high-quality Fabry–Pérot cavity. These realized record-low thresholds emanate from the high-quality on-chip cavity together with the core/crown@gradient-alloyed shell CQWs having giant gain cross-section and slow Auger rates. This microfabricated CQW laser provides a compact and inexpensive coherent light source for microfluidics and integrated optics covering the visible spectral region.


been proposed and utilized to broaden applications of these systems.^[4–7] The implementation of lasers in microfluidic networks to provide on-chip coherent/planar light sources is significantly important and desired since such implementation of lasers in microfluidic chips opens up a wide range of possibilities from optical detection to sensing which may lead to the development of fully automated chips.^[8–11] Microfluidic lasing and amplified spontaneous emission (ASE) using fluorescent dyes embedded in liquid–liquid waveguides have been reported in literature.^[12–16] Whitesides and co-workers reported multimode lasing from a liquid–liquid waveguide laser using Rhodamine 640 at 1.1 mJ cm⁻².^[15] Similarly, Chen and co-workers observed white lasing from Rhodamine 610, Courmarin 540, and Stilbene 420 at a threshold of 2.6 mJ cm⁻².^[16] The flow rates used in these devices had to be fast enough to decrease the residence time of the gain material^[15] to prevent photobleaching due to the irreversible conversion of them into nonfluorescent molecules caused by photon generation.^[17] The necessity of continuous replenishment of dye solutions at high flow rates requires sophisticated operation conditions such as external pumping and excess material consumption.

Microfluidics is an emerging technology for biological applications, including diagnostics and drug delivery.^[1] Owing to its ability to manipulate liquids at the microscale, microfluidics have the potential to introduce new routes for chemical synthesis, biological analysis, sensing, and cellular analysis, which require higher resolutions and lower detection limits than bulk systems.^[2,3] To date many improvements and components have

CQWs, which make a prominent class of colloidal nanocrystals (NCs) with favorable properties, such as large absorption cross-section,^[18] giant modal gain,^[19] large gain cross-section,^[20]

J. Maskoun, Dr. N. Gheshlaghi, F. Isik, Dr. S. Delikanli, Dr. O. Erdem, Prof. E. Y. Erdem, Prof. H. V. Demir
UNAM Institute of Materials Science and Nanotechnology
Bilkent University
Ankara 06800, Turkey
E-mail: yeganerdem@bilkent.edu.tr; volkan@bilkent.edu.tr

Dr. S. Delikanli, Prof. H. V. Demir
LUMINOUS! Center of Excellence for Semiconductor
Lighting and Displays
School of Electrical and Electronic Engineering
Nanyang Technological University
50 Nanyang Avenue, Singapore 639798, Singapore

 The ORCID identification number(s) for the author(s) of this article can be found under <https://doi.org/10.1002/adma.202007131>.

Dr. S. Delikanli, Prof. H. V. Demir
Division of Physics and Applied Physics
School of Physical and Mathematical Sciences
Nanyang Technological University
21 Nanyang Link, Singapore 639798, Singapore

Dr. O. Erdem, Prof. H. V. Demir
Department of Electrical and Electronics Engineering
Department of Physics
Bilkent University
Ankara 06800, Turkey
Prof. E. Y. Erdem
Department of Mechanical Engineering
Bilkent University
Ankara 06800, Turkey

DOI: 10.1002/adma.202007131

slow Auger recombination^[20–22] and narrow emission linewidth,^[23] have been widely utilized for optical gain and lasing applications.^[24,25] These properties, especially large gain cross-section and slow Auger recombination, make CQWs suitable for their utilization in lasers as optical gain media^[24] with lasing thresholds as low as $75 \mu\text{J cm}^{-2}$.^[20] Moreover, the high photostability of CQWs^[20,26] may allow for lasing from capillary-filled microfluidic devices, which is not possible by using dyes due to their bleaching in static solutions. CQWs in solution have a lower volume fraction than close-packed films of theirs, which makes the realization of in-solution lasers from CQWs challenging.^[27] Few studies have demonstrated solution-based lasing and gain from NCs with lasing thresholds on the order of tens of mJ cm^{-2} using cylindrical and spherical microcavities of optical fibers and microdrops, respectively, to create whispering gallery mode (WGM) lasers by confining light at their concave boundaries.^[28–30] However, the reported thresholds are high due to the lower gain cross-section of the employed nanocrystals, three orders of magnitude lower than those of CQWs.^[27,30]

Here, optical gain and single-mode lasing from CdSe/CdS@Cd_{1-x}Zn_xS core/crown@gradient-alloyed shell CQWs in solution are demonstrated in a microfluidic platform for the first time with a record low gain threshold in solution-based lasing from nanocrystals. In this work, unlike the previous reports of solution-based lasers a Fabry–Pérot cavity inside microchannel provides optical feedback through highly reflective designed mirrors to generate lasing action. CdSe/CdS@Cd_{1-x}Zn_xS core/crown@gradient-alloyed shell CQWs were inserted into the channel from an inlet using capillary forces. Since this microfluidic platform exhibiting lasing does not require external pumping, it has the advantage of stability and ease of operation.

The microfluidic devices used in this study are made of poly(dimethylsiloxane) (PDMS) to provide an easy integration of the laser to existing microfluidic functionalities. The 4 mm

long devices with 300 μm width and 100 μm height were prepared by soft lithography technique, where patterns from a silicon substrate were transferred to a PDMS mold (see the Supporting Information). For lasing action, a Fabry–Pérot cavity was created by depositing mirrors of different reflectance values on the walls of the microfluidic channels using thermal evaporation. The devices were finally sealed with a flat PDMS layer using O₂ plasma bonding. Then, a pipette tip was inserted into the channel inlet to fill the cavity with CQW solution. A laser was directed along the microchannel to induce optical gain as shown in the schematic in Figure 1a and the optical output was collected from the partially reflective mirror side as depicted in Figure 1b.

CdSe/CdS@Cd_{1-x}Zn_xS core/crown@gradient-alloyed shell CQWs, which have been previously reported by our group,^[31] are used as the gain medium in this work. Photoluminescence and absorption spectra of the synthesized core/crown@gradient-alloyed shell CQWs having three monolayers of Cd_{1-x}Zn_xS shell are presented in Figure 1c. Photoluminescence emission peaks at 633 nm and exhibits a linewidth of ≈ 25 nm. The inset in Figure 1c shows the transmission electron microscopy (TEM) image of the CQWs having lateral dimensions of 26 nm by 14 nm. Our CQWs were dispersed in toluene, which is normally incompatible with PDMS due to its swelling capacities.^[32] To address this issue and render our PDMS structure compatible with toluene, the ratio of curing agent to PDMS was increased from 1:10 to 1:5 and devices were thermally treated on a 200 °C hot plate for 24 h.^[33] Following the thermal treatment, mirrors were deposited to create an FP cavity prior to the plasma bonding. The method of introduction of the CQWs to the channel relies on capillary forces, which have the advantage of eliminating the need for external pumping. To justify the capillary action, the contact angle of toluene on treated PDMS was measured. According to the Young Laplace equation, the results show that capillary forces are large enough to induce flow (see the Supporting Information for details).

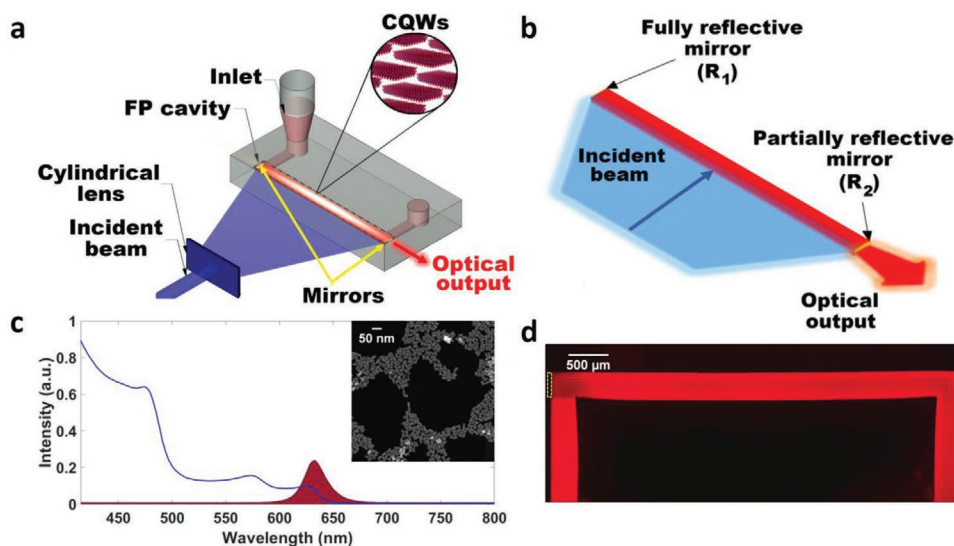


Figure 1. a) Design and operation of a microfluidic waveguide of CQWs, in which a FP cavity is created by the deposition of two mirrors on the channel walls. An external pump laser is used to induce excitation in the cavity. b) Illustration of the Fabry–Pérot (FP) cavity showing the mirrors and optical output. c) Absorption (blue) and PL (red) spectra of the CQWs used in this work, and the inset shows the TEM image of the CQWs. d) Fluorescence microscopy image of a filled channel.

After the thermal treatment of the pattern holding PDMS substrates, the Fabry–Pérot cavity was created by depositing mirrors on the walls of the microfluidic devices using a thermal evaporator. The mirrors on the channel walls were deposited by tilting the PDMS replica in the deposition chamber. For our experiments, the PDMS replicas were placed at a 75° angle using holders made of PDMS, as shown in Figure S2 in the Supporting Information. The reverse sides of the PDMS replica were plasma bonded to glass in order to prevent excess bending of PDMS and consequently avoid thin film damage. To obtain smooth mirror films on PDMS, the deposition of an adhesion layer of titanium or chromium is required^[34] and increasing the adhesion layer thickness enhances the smoothness of the thin films deposited on PDMS.^[35] In the visible wavelength range, Ag, Au, and Al are the most widely used as reflective materials with Ag having the best performance.^[36,37] However, Ag films oxidize in ambient conditions which results in significant reduction in their reflectivity over time. To overcome this issue, a thin layer of SiO₂ was deposited to protect the Ag film and increase its durability. The mirrors were deposited in a thermal evaporator chamber using 20 nm of Cr as the adhesion layer and 70 and 80 nm thick films of Ag for the reflective mirrors. The reflectance values of these mirrors are measured to be 93% and 95% for 70 and 80 nm thick Ag films, respectively (see the Experimental Section). Finally, 15 nm of SiO₂ was sputtered to prevent oxidation of the Ag films. Moreover, thin films were deposited on flat PDMS substrates for X-ray photoelectron spectroscopy (XPS) and reflectance characterizations. XPS was performed to identify the elemental composition of the fabricated mirrors and reflectance measurements were carried out to quantify the mirror performances.

The oxidation states of the mirror surfaces were investigated for bare Ag films and SiO₂ protected Ag films using XPS. Both samples were exposed to oxygen plasma in order

to mimic experimental conditions. The results for the mirror films without and with SiO₂ protective coating are presented in Figure 2a,b,d–f, respectively.

Figure 2a shows deconvolution of XPS silver peaks. Peak positions located at 368.8 and 368.2 eV correspond to Ag and Ag₂O, respectively, along with the absence of the satellite peak. Since AgO is notoriously unstable in ultrahigh vacuum, its presence cannot be confirmed nor rejected. Detailed scans of the O 1s region is also recorded but not very insightful because AgO contributions can overlap with carbonate groups from air contamination in the O 1s region (Figure 2b). The only definitive assignment that can be made in the O 1s spectrum in Figure 2b is the small peak at 529.9 eV, ascribed to Ag₂O. The larger peak at 531.5 eV of the O 1s spectrum could be ascribed to oxygen chemisorbed on a silver surface or Ag–O–Ag bonds.^[38] These results confirm the presence of an oxide layer on the surface of the unprotected Ag film.

As shown in Figure 2d, the Ag 3d_{5/2} and Ag 3d_{3/2} peaks were found at binding energies of 368.8 and 374.8 eV and satellite peaks at 372.6 and 378.6 eV, respectively. The combination of these peaks and splitting of 6.0 eV in Ag 3d doublet indicates that the silver species exist as Ag⁰ on the surface and the peaks corresponding to Ag⁺ cations are not found.^[39] The characteristic O 1s peak (Figure 2e) located at 532.5 eV is ascribed to the lattice O²⁻ of SiO₂ and presence of other components such as OH, H₂O, and carbonate species adsorbed onto the surface. Figure 2f displays the XPS spectrum of Si 2p. The peak located at 103.3 eV indicates that Si exists as SiO₂. These results confirm that the SiO₂ layer deposition successfully prevents the formation of the silver oxide layer.

These results imply the smooth and uniform quality of the deposited films on the PDMS substrate. A SEM image of the deposited mirror on the channel wall is provided in Figure 2c, and the inset shows a magnification of the thin film surface.

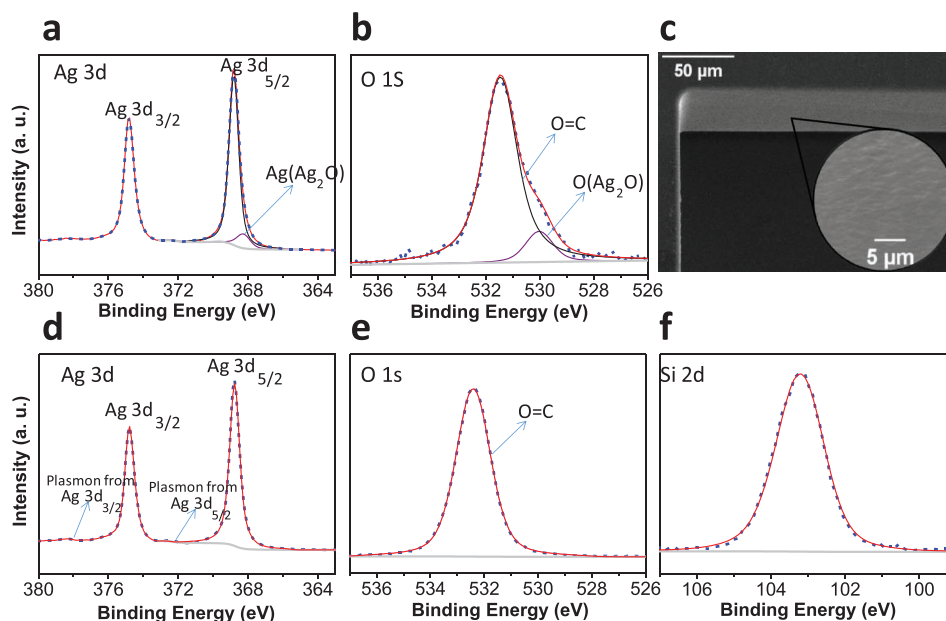


Figure 2. a,b,d–f) High-resolution XPS spectra of Ag 3d (a), O 1s (b), Ag 3d (d), O 1s (e), and Si 2p (f) of silver mirrors without (a,b) and with (d–f) oxidation protection layer of SiO₂ after oxygen plasma. c) SEM image of the microfluidic device showing the smooth mirror surface.

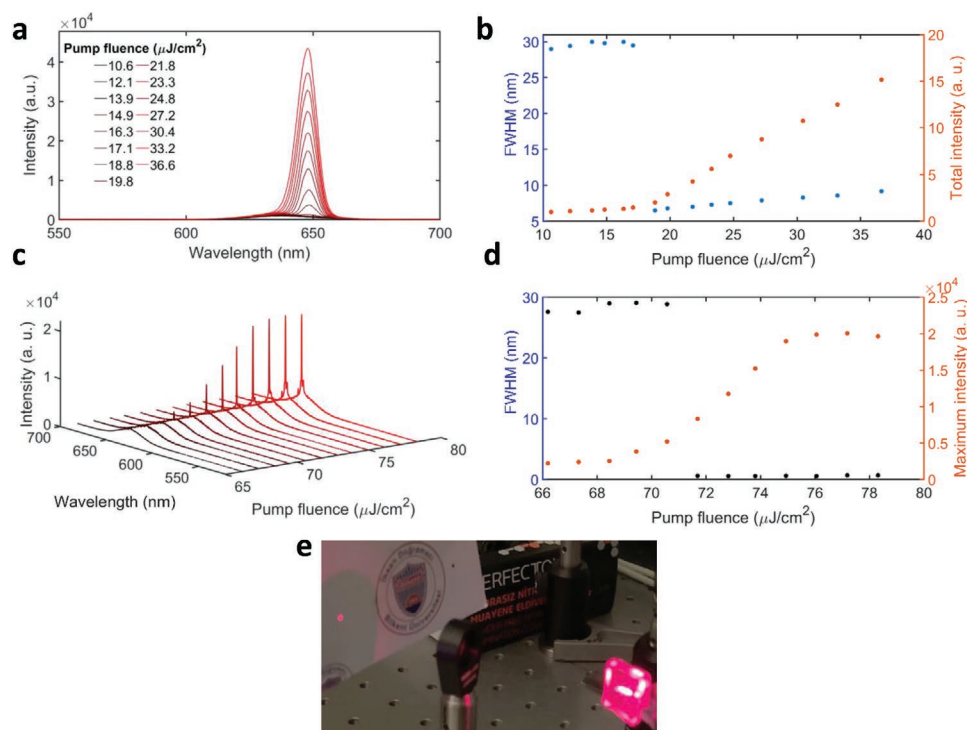


Figure 3. a) Photoluminescence spectra of CQWs in the microfluidic device under pulsed excitation at various pump intensities. b) Luminescence and linewidth versus pump fluence. c) Lasing of CQWs in microfluidic devices with mirrors. d) The output intensity of the device and linewidth values with increasing pump intensity. e) Image of the output laser beam focused onto a screen.

The absence of cracks on mirror surface further confirms the smoothness and uniformity of the deposited thin films.

To evaluate the optical gain of our CQWs in microchannels, mirrorless devices were filled with the core/crown@gradient-alloyed shell CQWs dispersed in toluene and then excited using one-photon absorption. The microchannels containing CQW solution were excited using femtosecond pulses (pulse width ≈ 120 fs) at 400 nm and 1 kHz repetition rate. A cylindrical lens was used to obtain excitation with a stripe geometry. Emitted photons were collected by using an optical fiber connected to a spectrometer. Toluene was used as a solvent in this work instead of usually used hexane, because of high boiling point and refractive index of the toluene compared to hexane and most of the other nonpolar solvents. The high boiling point of toluene (110.6 °C) prevents the possibility of particle aggregation due to the solvent evaporation in the channel. In addition, higher refractive index of toluene provides efficient confinement of the electrical field within the gain medium which is desirable for optical gain applications.

Spontaneous emission centered at 637.5 nm with an emission linewidth of 29.2 nm is observed from devices for pump fluences up to 17.1 $\mu\text{J cm}^{-2}$ as presented in Figure 3a. Increasing the pump fluence further results in the emergence of a sharp peak with a narrow emission linewidth of 6.8 nm centered around 648.1 nm, which is attributed to amplified spontaneous emission (ASE). This attribution is corroborated by the increase in the slope of the total intensity versus pump fluence curve beyond the threshold which is at 17.1 $\mu\text{J cm}^{-2}$ as can be seen in Figure 3b. Previously optical gain from core/shell CQWs were demonstrated using only two- and three-photon

pumping.^[27] This threshold of 17.1 $\mu\text{J cm}^{-2}$ from our designed CdSe/CdS@Cd_xZn_{1-x}S core/crown@gradient-alloyed shell CQW heterostructures exhibiting large modal gain^[20] and slow Auger recombination as a result of smooth confinement potential^[20,40] is almost an order of magnitude lower than the previously best threshold from solution based optical gain from colloidal nanocrystals of all kinds. The previously demonstrated best ASE threshold in solution is from perovskite nanocrystals with a threshold of 105 $\mu\text{J cm}^{-2}$. The redshift of ASE emission (≈ 10 nm) is due to the multiexcitonic gain commonly observed in type-I structures and is advantageous for lasing action since it reduces self-absorption and hence gain threshold.^[20,41]

For the fabrication of the lasing device, two mirrors were deposited to the ends of the microfluidic channel as described earlier. Similar to the operation conditions for the optical gain measurements, the solution of CQWs was introduced to the channels via capillary action and the channel was excited via one-photon absorption at 400 nm using stripe geometry by employing a cylindrical lens. At low pump intensities, spontaneous emission dominates the spectrum and has similar characteristics to the spontaneous emission observed before the onset of ASE in the optical gain measurement experiment as can be seen in Figure 3c. At a pump fluence of 68.4 $\mu\text{J cm}^{-2}$ and beyond, the transition from spontaneous emission to lasing is evident from the emergence of a narrow emission feature (FWHM of the lasing peak) along with superlinear increase in the output intensity with the increasing input pump intensity as can be seen in Figure 3c. The emission linewidth drops from 27.0 nm centered at 642.6 nm to 0.54 nm centered at 645.6 nm. This redshifted lasing action signifies the multiexcitonic

optical gain in our device. Figure 3c presents the device emission at various pump fluences and Figure 3d shows the drop in the linewidth with the emergence of lasing action. The quality factor (Q) of our cavity exhibiting single mode lasing at 645.6 nm with FWHM of 0.54 nm is ≈ 1195 . This high Q is due to the highly reflective and air stable Ag coated mirrors with SiO_2 protection layer designed for this work. At a pump fluence of $76.1 \mu\text{J cm}^{-2}$ and above, the laser emission saturates and results in the expected “S”-shaped behavior as shown in Figure 3d. This relatively quick saturation of the lasing output ($76 \mu\text{J cm}^{-2}$) observed right after the lasing threshold ($68 \mu\text{J cm}^{-2}$) can be attributed to the rapid increase in the modal gain with the increasing pump fluence along with the long optical path, together leading to depletion of the gain media quickly. The output laser beam focused onto a screen is shown in Figure 3e. The lasing threshold achieved in this work via single-photon pumping is three orders of magnitude lower than the lasing thresholds observed from other colloidal nanocrystals.^[28,30] In addition, in all previous demonstrations of lasing using solution of colloidal nanocrystals multimode lasing was demonstrated and single-mode lasing has not been demonstrated.^[28–30] This is also one of the reason for such high lasing thresholds in the other demonstrations along with the lower modal gain of QDs and nanorods compared to QWs^[19] and slow Auger rates in our CQWs having smooth confinement potential.^[20,40] The achievement of single mode lasing in our device can be attributed to the mode competition. Each mode will have different modal gain since the modal gain varies strongly within the bandwidth of the optical gain as demonstrated previously.^[19] As a result, the mode having the largest modal gain outcompetes the other modes supported by the cavity, allowing for a single-mode lasing action for the pump fluence range we investigated.

The ultralow threshold of single-mode lasing in our work also ensures the stability of lasing since such high fluences used in previous works will likely promote evaporation of the solvents as observed and deterioration of the nanocrystals^[29] and as a result diminish the lifetime and stability of these device. Irreversible blueshift of the of the gain profile was observed in QD microdrop lasers as a result of such high fluences (three orders of magnitude stronger than the fluences in this work) leading photo-oxidation.^[29] This is likely the reason of very few reports on solution based lasing. This makes our ultralow threshold single-mode lasing is significantly important and our demonstration in here can pave the way for realization of practical microfluidic lasers based on colloidal CQWs. Also, it is worth mentioning that few more modes emerge with lower intensity in our microfluidic laser at higher fluences as can be seen in Figure 3c as they overcome the losses in the cavity at higher fluences.

In summary, we have demonstrated an ultralow threshold single-mode laser built in a PDMS microfluidic structure using $\text{CdSe/CdS}@_{\text{Cd}_x\text{Zn}_{1-x}}\text{S}$ core/crown@gradient-alloyed shell CQWs dispersed in toluene as the gain medium. Owing to the photostability of the core/crown@gradient-alloyed shell CQWs solution and the strong capillary interaction with PDMS, an easy to operate in-solution laser was achieved using a minimal amount of the gain material. This is the first achievement of single-mode in-solution laser from colloidal nanocrystals with

record low threshold, which is three orders of magnitude better than previous multimode in-solution lasers from colloidal nanocrystals. Such an ultralow threshold, which is due to the giant gain cross-section and slow Auger rate in these core/crown@gradient-alloyed shell CQWs, is significantly important for realization of practical microfluidic lasers. The fabricated microfluidic device may be extended to contain multiple channels, each filled with a different ensemble of colloidal NCs emitting in different colors, thereby paving the way for the development of easy-to-operate low-threshold white lasers in solution. Therefore, our capillary microfluidic in solution laser provides a foundation to explore a rich variety of low cost, broadband light sources, which can be easily integrated to existing microfluidic devices. The remarkably low lasing threshold obtained with the in-solution CQWs can also help their utilization in laminar-flow lasers, which enable tuning the output laser beam and cavity parameters during the operation.

Supporting Information

Supporting Information is available from the Wiley Online Library or from the author.

Acknowledgements

The authors gratefully acknowledge the financial support in part from Singapore National Research Foundation under the programs of NRF-NRFI2016-08 and the Science and the Singapore Agency for Science, Technology and Research (A*STAR) SERC Pharos Program under Grant No. 152-73-00025 and in part from TUBITAK 115F297, 117E713, and 119N343. H.V.D. also acknowledges support from TUBA.

Conflict of Interest

The authors declare no conflict of interest.

Keywords

microfluidics, semiconductor quantum wells, solution lasing, solution optical gain

Received: October 19, 2020

Revised: December 10, 2020

Published online: January 25, 2021

- [1] H. A. Santos, D. Liu, H. Zhang, *Microfluidics for Pharmaceutical Applications: From Nano/Micro Systems Fabrication to Controlled Drug Delivery*, Elsevier, Amsterdam, The Netherlands **2019**.
- [2] G. M. Whitesides, *Nature* **2006**, *442*, 368.
- [3] B. Kuswandi, J. Huskens, W. Verboom, *Anal. Chim. Acta* **2007**, *601*, 141.
- [4] H. Fallahi, J. Zhang, H. P. Phan, N. T. Nguyen, *Micromachines* **2019**, *10*, 830.
- [5] O. Scheler, W. Postek, P. Garstecki, *Curr. Opin. Biotechnol.* **2019**, *55*, 60.
- [6] H. Yang, M. A. M. Gijjs, *Chem. Soc. Rev.* **2018**, *47*, 1391.

- [7] N. Convery, N. Gadegaard, *Micro Nano Eng.* **2019**, *2*, 76.
- [8] C. Monat, P. Domachuk, B. J. Eggleton, *Nat. Photonics* **2007**, *1*, 106.
- [9] F. Ghasemi, A. A. Eftekhar, D. S. Gottfried, X. Song, R. D. Cummings, A. Adibi, *Proc. SPIE* **2013**, *8594*, 85940A.
- [10] D. Kim, P. Popescu, M. Harfouche, J. Sendowski, M. E. Dimtsantou, R. C. Flagan, A. Yariv, *Opt. Lett.* **2015**, *40*, 4106.
- [11] Y. Sun, X. Fan, *Angew. Chem., Int. Ed.* **2012**, *51*, 1236.
- [12] H. Zhang, Y. Sun, *Opt. Express* **2018**, *26*, 11284.
- [13] Z. Li, Z. Zhang, T. Emery, A. Scherer, D. Psaltis, *Opt. Express* **2006**, *14*, 696.
- [14] Y. Cheng, K. Sugioka, K. Midorikawa, *Opt. Lett.* **2004**, *29*, 2007.
- [15] D. V. Vezenov, B. T. Mayers, R. S. Conroy, G. M. Whitesides, P. T. Snee, Y. Chan, D. G. Nocera, M. G. Bawendi, *J. Am. Chem. Soc.* **2005**, *127*, 8952.
- [16] Y. Kong, H. Dai, X. He, Y. Zheng, X. Chen, *Opt. Lett.* **2018**, *43*, 4461.
- [17] R. Zondervan, F. Kulzer, M. A. Kol'chenk, M. Orrit, *J. Phys. Chem. A* **2004**, *108*, 1657.
- [18] A. Yeltik, S. Delikanli, M. Olutas, Y. Kelestemur, B. Guzelurk, H. V. Demir, *J. Phys. Chem. C* **2015**, *119*, 26768.
- [19] B. Guzelurk, M. Pelton, M. Olutas, H. V. Demir, *Nano Lett.* **2019**, *19*, 277.
- [20] N. Taghipour, S. Delikanli, S. Shendre, M. Sak, M. Li, F. Isik, I. Tanriover, B. Guzelurk, T. C. Sum, H. V. Demir, *Nat. Commun.* **2020**, *11*, 3305.
- [21] L. T. Kunneman, M. D. Tessier, H. Heuclin, B. Dubertret, Y. V. Aullin, F. C. Grozema, J. M. Schins, L. D. A. Siebbeles, *J. Phys. Chem. Lett.* **2013**, *4*, 3574.
- [22] Y. Altintas, K. Gungor, Y. Gao, M. Sak, U. Quliyeva, G. Bappi, E. Mutlugun, E. H. Sargent, H. V. Demir, *ACS Nano* **2019**, *13*, 10662.
- [23] S. Ithurria, M. D. Tessier, B. Mahler, R. P. S. M. Lobo, B. Dubertret, A. L. Efros, *Nat. Mater.* **2011**, *10*, 936.
- [24] B. Guzelurk, Y. Kelestemur, M. Olutas, S. Delikanli, H. V. Demir, *ACS Nano* **2014**, *8*, 6599.
- [25] M. Olutas, B. Guzelurk, Y. Kelestemur, A. Yeltik, S. Delikanli, H. V. Demir, *ACS Nano* **2015**, *9*, 5041.
- [26] M. Sak, N. Taghipour, S. Delikanli, S. Shendre, I. Tanriover, S. Foroutan, Y. Gao, J. Yu, Z. Yanyan, S. Yoo, C. Dang, H. V. Demir, *Adv. Funct. Mater.* **2020**, *30*, 1907417.
- [27] M. Li, M. Zhi, H. Zhu, W. Y. Wu, Q. H. Xu, M. H. Jhon, Y. Chan, *Nat. Commun.* **2015**, *6*, 8513.
- [28] M. Kazes, D. Y. Lewis, Y. Ebenstein, T. Mokari, U. Banin, *Adv. Mater.* **2002**, *14*, 317.
- [29] J. Schäfer, J. P. Mondia, R. Sharma, Z. H. Lu, A. S. Susha, A. L. Rogach, L. J. Wang, *Nano Lett.* **2008**, *8*, 1709.
- [30] Y. Wang, K. S. Leck, V. D. Ta, R. Chen, V. Nalla, Y. Gao, T. He, H. V. Demir, H. Sun, *Adv. Mater.* **2015**, *27*, 169.
- [31] S. Shendre, S. Delikanli, M. Li, D. Dede, Z. Pan, S. T. Ha, Y. H. Fu, P. L. Hernández-Martínez, J. Yu, O. Erdem, A. I. Kuznetsov, C. Dang, T. C. Sum, H. V. Demir, *Nanoscale* **2019**, *11*, 301.
- [32] J. N. Lee, C. Park, G. M. Whitesides, *Anal. Chem.* **2003**, *75*, 6544.
- [33] M. Kim, Y. Huang, K. Choi, C. H. Hidrovob, *Microelectron. Eng.* **2014**, *124*, 66.
- [34] S. P. Lacour, in *Stretchable Electronics* (Ed: T. Someya), John Wiley and Sons, Hoboken, NJ, USA **2012**, Ch. 4.
- [35] O. Graudejus, P. Görrn, S. Wagner, *ACS Appl. Mater. Interfaces* **2010**, *2*, 1927.
- [36] G. Hass, *J. Opt. Soc. Am.* **1982**, *72*, 27.
- [37] J. B. Heaney, L. K. Kauder, S. C. Freese, M. A. Quijada, *Proc. SPIE* **2012**, *8510*, 85100F.
- [38] N. J. Firet, M. A. Blommaert, T. Burdyny, A. Venugopal, D. Bohra, A. Longo, W. A. Smith, *J. Mater. Chem. A* **2019**, *7*, 2597.
- [39] J. Feng, D. Fan, Q. Wang, L. Ma, W. Wei, J. Xie, J. Zhu, *Colloids Surf., A* **2017**, *520*, 743.
- [40] G. E. Cragg, A. L. Efros, *Nano Lett.* **2010**, *10*, 313.
- [41] C. Dang, J. Lee, C. Breen, J. S. Steckel, S. Coe-Sullivan, A. Nurmikko, *Nat. Nanotechnol.* **2012**, *7*, 335.